Microstructure and growth mechanism of epitaxial $SrRuO_3$ thin films on (001) $LaAlO_3$ substrates

J. C. Jiang and X. Q. Pan[a]
Department of Materials Science and Engineering, The University of Michigan, Ann Arbor, Michigan 48109

(Received 17 July 2000; accepted for publication 5 March 2001)

$SrRuO_3$ thin films deposited on (001) $LaAlO_3$ substrates by 90° off-axis sputtering at 600 °C were studied by atomic force microscopy (AFM) and transmission electron microscopy (TEM). Both AFM and cross-section TEM investigations show that the films have a rough surface. Plan-view TEM studies demonstrate that the films are composed of all three different types of orientation domains (twins). These domain structures and surface morphology are different from the $SrRuO_3$ film deposited on the (001) $SrTiO_3$ substrate which has an atomically flat surface and is composed of only the [110]-type domains. The reason for these differences was ascribed as the effect of lattice mismatch across the film/substrate interface. It is proposed that a $SrRuO_3$ thin film grows on a (001) $SrTiO_3$ substrate through a two-dimensional nucleation process, while a film on $LaAlO_3$ grows with three steps: the coherent growth of a few monolayers at the initial stage through a two-dimensional nucleation process; the formation of misfit dislocations when the film reaches a critical thickness; and an island-like growth thereafter due to the nonuniform distribution of stress along the film surface. © *2001 American Institute of Physics.* [DOI: 10.1063/1.1368160]

I. INTRODUCTION

Epitaxial strontium ruthenate ($SrRuO_3$) thin films have an attractive prospect for applications as electrodes for nonvolatile ferroelectric memory devices,[1] superconductor-normal-superconductor Josephson junctions, and dielectric constant capacitors,[2–4] due to their high thermal conductivity and stability, high resistance to chemical corrosion,[5] high-perpendicular remnant magnetization, and large magneto-optical constant.[6] The properties of $SrRuO_3$ thin films vary with the growth conditions such as substrate miscut. For instance, the $SrRuO_3$ thin films deposited on (001) $SrTiO_3$ and (001) $LaAlO_3$ (pseudo-cubic indices are used hereafter) show different coercive behavior at low temperature.[5] A strong anisotropic magnetoresistance in the $SrRuO_3$ thin films grown on miscut (001) $SrTiO_3$ substrates and identical magnetoresistance behavior in two orthogonal directions on the film grown on (001) $LaAlO_3$ substrate were observed.[7]

The difference in properties was ascribed to the different microstructures of thin films which are determined by growth conditions. Microstructures of $SrRuO_3$ thin films grown on (001) $SrTiO_3$ substrates have been studied recently by x-ray diffraction[8] and transmission electron microscopy (TEM).[9,10] It was found that the $SrRuO_3$ thin films grown on (001) $SrTiO_3$ substrates showed very smooth surface and very sharp interface between the thin film and the substrate.[9] Furthermore, the $SrRuO_3$ thin films grown on the exact (001) $SrTiO_3$ substrate had two (110)-type orientation domains, whereas the films grown on the vicinal (001) $SrTiO_3$ substrates were composed of a single (110) domain structure.[8–10] However, the microstructure of $SrRuO_3$ thin films grown on (001) $LaAlO_3$ substrates is so far unclear. In this work, the microstructure and surface morphology of the $SrRuO_3$ thin films grown on (001) $LaAlO_3$ are reported.

$SrRuO_3$ is an orthorhombic phase with lattice parameters $\boldsymbol{a}=5.5670$ Å, $\boldsymbol{b}=5.5304$ Å, and $\boldsymbol{c}=7.8446$ Å.[11] The room temperature phase of $LaAlO_3$ has a rhombohedral structure with a primitive lattice of $\boldsymbol{a}_R=5.357$ Å, $\alpha_R=60.1°$, and a corresponding hexagonal cell of $\boldsymbol{a}_H=5.365$ Å, $\boldsymbol{c}_H=13.11$ Å.[12] This structure can also be described in terms of a pseudo-cubic lattice with a constant of $\boldsymbol{a}_C=3.790$ Å. (All the planes and directions of $LaAlO_3$ referred to in this work are based on the pseudo-cubic unit cell.) The periods of [110], $[1\bar{1}0]$, and [001] of $SrRuO_3$ are about twice the constant of the pseudo-cubic lattice of $LaAlO_3$. When $SrRuO_3$ grows on the (001) $LaAlO_3$ substrate, the [110], $[1\bar{1}0]$, or [001] direction of $SrRuO_3$ can be aligned parallel to either [100] or [010] in the $LaAlO_3$ (001) surface. Therefore, a total of six different types of orientation domains can be possibly formed in the film based on the $SrRuO_3/LaAlO_3$ interfacial structural models. The orientation relationships between different $SrRuO_3$ domains in the film and the (001) $LaAlO_3$ substrate, which are similar to those for the $SrRuO_3$ film grown on exact (001) $SrTiO_3$ substrates as reported previously,[10] can be summarized as

$$(110)_{SRO}\|(001)_{LAO},\,[001]_{SRO}\|[010]_{LAO},\quad \text{and}\,[\bar{1}10]_{SRO}\|[100]_{LAO}(\text{mode}\,\mathbf{X});$$

$$(110)_{SRO}\|(001)_{LAO},\,[001]_{SRO}\|[100]_{LAO},\quad \text{and}\,[1\bar{1}0]_{SRO}\|[010]_{LAO}(\text{mode}\,\mathbf{Y});$$

$$(\bar{1}10)_{SRO}\|(001)_{LAO},\,[001]_{SRO}\|[010]_{LAO},\quad \text{and}\,[110]_{SRO}\|[100]_{LAO}(\text{mode}\,\mathbf{X}');$$

[a]Electronic mail: panx@umich.edu

 © 2001 American Institute of Physics

$(\bar{1}10)_{SRO} \| (001)_{LAO}, [001]_{SRO} \| [100]_{LAO},$

and $[\bar{1}\bar{1}0]_{SRO} \| [010]_{LAO}$(mode $\mathbf{Y}'$);

$(001)_{SRO} \| (001)_{LAO}, [100]_{SRO} \| [110]_{LAO},$

and $[010]_{SRO} \| [1\bar{1}0]_{LAO}$(mode $\mathbf{Z}$);

$(001)_{SRO} \| (001)_{LAO}, [100]_{SRO} \| [\bar{1}10]_{LAO},$

and $[010]_{SRO} \| [110]_{LAO}$(mode $\mathbf{Z}'$).

Because of the pseudo-cubic characteristic of the $SrRuO_3$ structure, the difference between the X (Y or Z) and X′ (Y′ or Z′) is not distinguishable by means of conventional TEM. Thus, only $\mathbf{X}(\mathbf{X}')$, $\mathbf{Y}(\mathbf{Y}')$, and $\mathbf{Z}(\mathbf{Z}')$-type domains can be distinguished in this work.

II. EXPERIMENTAL METHODS

$SrRuO_3$ thin films on (001) $LaAlO_3$ were deposited by 90° off-axis rf sputtering at 600 °C. Atomic force microscopy (AFM) studies were carried out in a Digital Instrument Nanoscope III. For cross-section TEM studies the $SrRuO_3/LaAlO_3$ samples were cut along the [100] direction of $LaAlO_3$. The cut slides were glued face to face by joining the $SrRuO_3$ surfaces. Plan-view and cross-section TEM specimens were prepared by mechanical grinding, polishing, and dimpling, followed by Ar-ion milling. Conventional diffraction contrast images were obtained using a Philips CM12 electron microscope operated at 120 kV. High-resolution transmission electron microscopy (HRTEM) observations were carried out in a JEOL 4000EX electron microscope operated at 400 kV with a point resolution of 0.17 nm.

III. EXPERIMENTAL RESULTS

The surface morphology of thin films was investigated using both AFM and cross-section TEM techniques. Figure 1(a) is an AFM image of the $SrRuO_3$ thin film grown epitaxially on the (001) $LaAlO_3$ substrate. It shows that the film has a rough surface with a root mean square roughness of 47 nm. Figure 1(b) is a cross-sectional TEM image taken from the same film. The surface roughness determined from this cross-sectional TEM image is in agreement with that obtained from the AFM studies. Figure 1(c) is a cross-section dark-field TEM image taken from a $SrRuO_3$ thin film which was deposited under the same conditions, but on (001) $SrTiO_3$ substrate. The regions with high and low intensities represent the orientation domains (twins) of two different types (X and Y), as reported previously.[8–10] It is seen that the $SrRuO_3$ thin film grown on (001) $SrTiO_3$ substrate has nearly atomically flat surface. In contrast, the $SrRuO_3$ film grown on the (001) $LaAlO_3$ substrate has a rough surface with a sinusoidal-like modulation [Fig. 1(b)], although the growth conditions were the same except for different substrate materials. The wavelength of the surface roughness is about 200 nm, determined from both cross-sectional TEM and AFM images.

Selected area electron diffraction and dark-field contrast image studies of epitaxial $SrRuO_3$ thin films on the (001) $LaAlO_3$ substrate show that the $SrRuO_3$ thin films consist of the orientatiaon domains of all the three types. Figure 2(a) is a selected area electron diffraction pattern taken from a plan-view sample. This pattern is a superposition of diffraction patterns of all the three types of domains, i.e., one [001] zone and two [110] zone diffraction patterns which are rotated by 90° around the [110] zone axis with respect each other. The weak reflections marked by α, β, and γ in Fig. 2(a) belong to two different [110] zone diffraction patterns and the [001] zone diffraction pattern, respectively. The dark-field diffraction contrast images in Figs. 2(b) and 2(c) were formed, respectively, using α and β weak reflections in Fig. 2(a). Thus, regions with high intensity in Fig. 2(b) represent the [110]-oriented domains (X type) whereas bright regions in Fig. 2(c) represent the $[1\bar{1}0]$-oriented domains (Y type). Figure 2(d) is a dark-field image formed using the γ weak reflection in Fig. 2(a). Accordingly, regions with high intensity correspond to the [001]-oriented domains (Z type). The fine dark fringes existing in the dark-field images correspond to antiphase boundaries of $SrRuO_3$. All three types of orientation domains are distributed randomly in the film and have a mean size of about 150 nm in diameter. Over the entire plan-

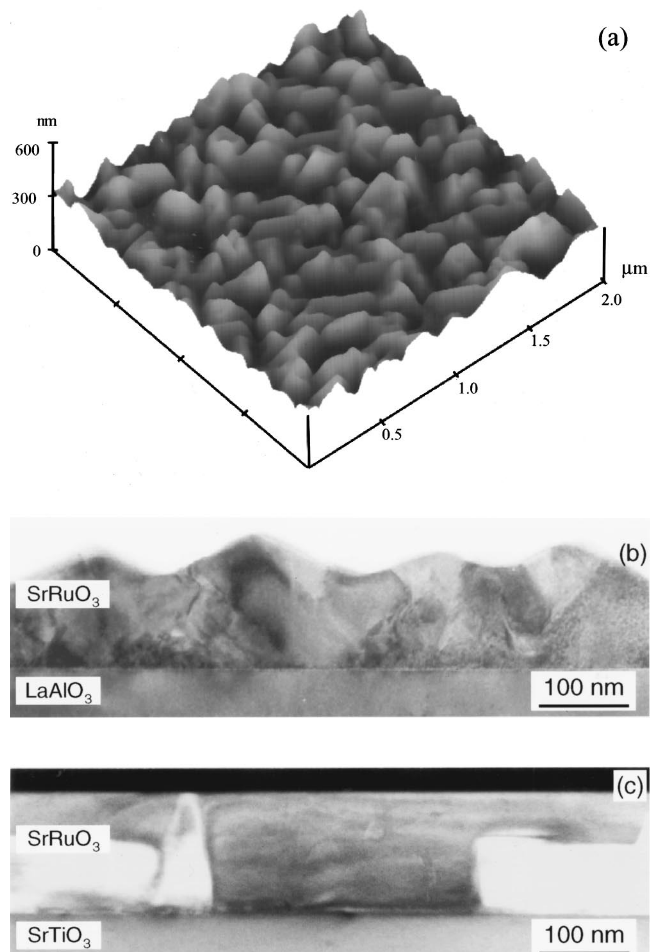

FIG. 1. (a) AFM image of a $SrRuO_3$ thin film grown on (001) $LaAlO_3$ substrate showing a rough surface. (b) Cross-section TEM image of the thin film showing the sinusoidal modulation of film surface. (c) Cross-section dark-field TEM image taken from a $SrRuO_3$ thin film which was deposited under the same conditions, but on (001) $SrTiO_3$ substrate.

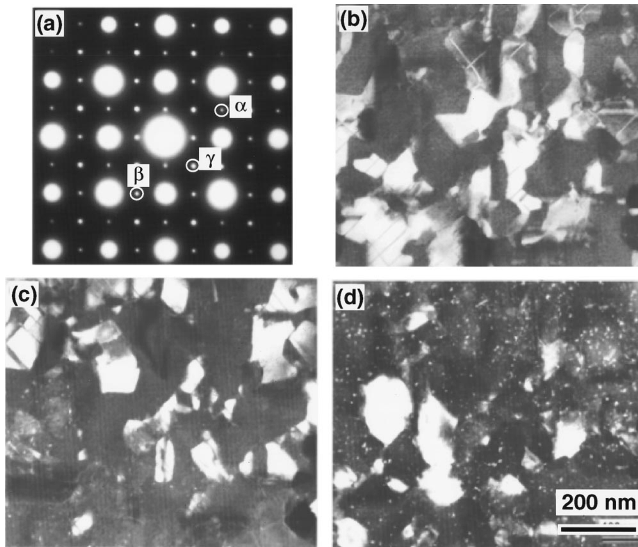

FIG. 2. (a) Selected area electron diffraction pattern taken from a plan-view specimen, (b), (c), and (d) dark-field images using weak reflections marked by ''α,'' ''β,'' and ''γ'' in (a), respectively.

view samples, the three types of domains have nearly the same volume fraction.

The orientation domains of all the three types observed in plan-view samples were also confirmed by cross-section TEM studies. In addition to the existence of orientation domains, misfit dislocations were also observed at the interfaces between the substrate and the film due to the lattice mismatch. Figure 3 is a dark-field image formed using the (202) reflection of a cross-sectional sample, showing the presence of misfit dislocations along the film/substrate interfaces. The misfit dislocations have nearly equal spacing along the interface, which suggests that the $SrRuO_3/LaAlO_3$ interface is semicoherent.

Figure 4 is a high-resolution TEM micrograph of the $SrRuO_3/LaAlO_3$ interface taken from the same cross-sectional specimen as for Fig. 3. The incident electron beam is parallel to the [010] direction of the $LaAlO_3$ substrate. A misfit dislocation is seen in the middle of the image. The Burgers vector of the dislocation corresponds to [100] of $SrRuO_3$, determined by the Burgers circuit as shown in Fig. 4. The dashed line in the middle of the image indicates the position of the $SrRuO_3/LaAlO_3$ interfface. It can be seen that the misfit dislocation is not exactly located at the

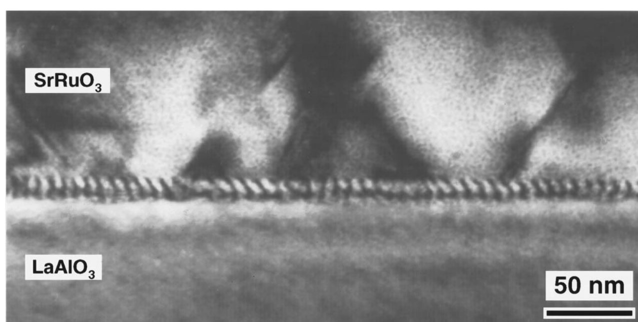

FIG. 3. Dark-field image using (202) reflection taken from a cross-section sample showing periodically distributed misfit dislocations at interface.

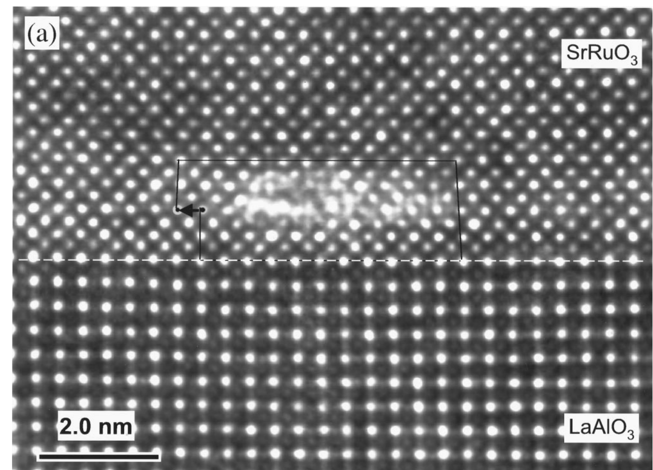

FIG. 4. HRTEM image showing the $SrRuO_3/LaAlO_3$ interfacial structure. Dashed line indicates the position of the interface.

$SrRuO_3/LaAlO_3$ interface, but in the $SrRuO_3$ thin film a few monolayers away from the interface. This characteristic is true for most of misfit dislocations observed.

IV. DISCUSSIONS

The microstructure and surface morphology of the $SrRuO_3$ thin films grown on (001) $LaAlO_3$ substrates are different from that of the films grown on (001) $SrTiO_3$ substrates under the otherwise same deposition conditions which were studied in the previous work.[9,10] Comparing the present results with those previous reported,[13] one can find that while an atomically flat $SrRuO_3$ film can be grown on a (001) $SrTiO_3$ substrate, when $SrTiO_3$ is replaced by $LaAlO_3$ the film surface becomes rough and an island-like growth process is observed. These phenomena are similar to that observed in highly strained InGaAs films grown on GaAs.[14]

$SrRuO_3$ has a pseudo-cubic perovskite structure which is distorted from the ideal cubic perovskite structure by tilting the RuO_6 octahedra with a lattice parameter of about 3.93 Å.[15,16] The lattice mismatch between the $SrRuO_3$ thin film and the $LaAlO_3$ substrate is about 3.7% in comparison with a small lattice mismatch of about 0.64% between the $SrRuO_3$ film and the $SrTiO_3$ substrate which has the cubic perovskite structure with a lattice constant of 3.905 Å. In consideration of the fact that the $SrRuO_3$ films on both substrates were deposited otherwise under the same condition, the lattice mismatch between the film and the $LaAlO_3$ substrate should be responsible for the difference in the microstructure and surface morphology of the films. For such a system with a high degree of lattice mismatch, it is believed that there is no net driving force for two-dimensional (2D) flat film growth. As a result, the film growth proceeds through a three-dimensional island-like growth process. Srolovitz predicted the instability of the flat surface of highly stressed solid films with respect to perturbations with wavelength greater than a critical value, based on a simple linear stability analysis.[17] The predicted wavelength of the instability is consistent with observations of thin InGaAs films grown on GaAs.

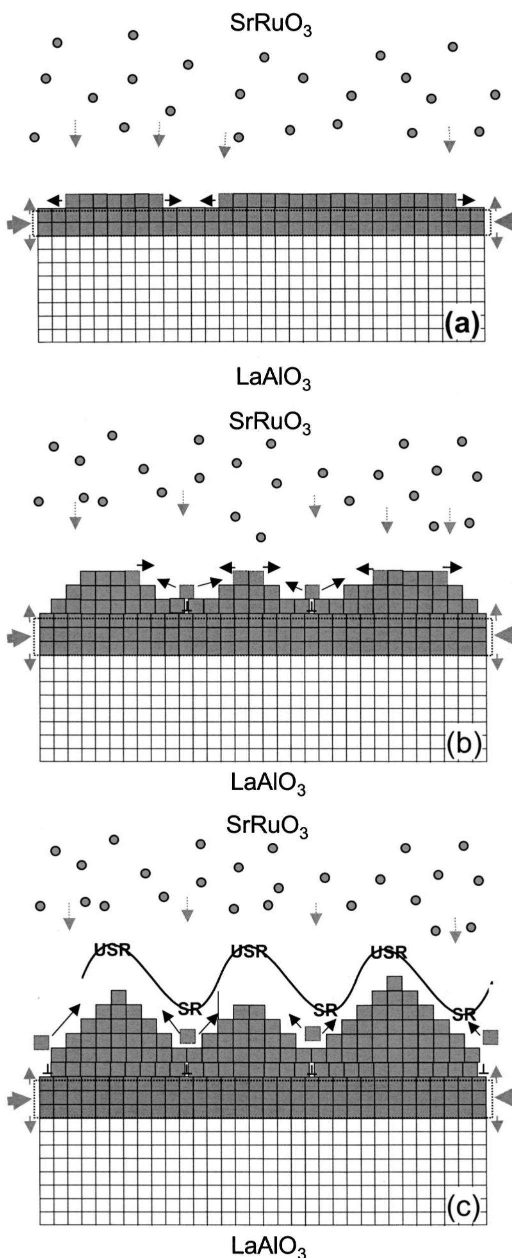

FIG. 5. Schematics showing the growth mechanisms of $SrRuO_3$ thin films on the (001) $LaAlO_3$ substrate. (a) Formation of a coherent epitaxial layer with a thickness of several monolayers at the initial stage of film growth; (b) misfit dislocations form when the film growth reaches a critical thickness. (c) Formation of an island-like surface morphology due to the mass transport in the film surface from the stressed regions (SR) to unstressed regions (USR).

In the initial growth stage, since the $SrRuO_3$ film is as thin as only a few monolayers it may grow coherently epitaxially on the (001) $LaAlO_3$ substrate with a 2D nucleation process [Fig. 5(a)]. The stress at this stage is not readily relaxed due to the extremely small film thickness. The film is strongly compressed due to the small lattice constant of $LaAlO_3$ in comparison with that of $SrRuO_3$. With further growth, the stress could be relaxed by the formation of misfit dislocations in the film [Fig. 5(b)]. Since the misfit dislocations are formed after a coherent epitaxial layer is grown, they appear a few monolayers away from the film/substrate interface. This configuration of misfit dislocations is seen in the HRTEM image [Fig. 4]. After the formation of misfit dislocations the distributions of stress in the film surface is nonuniform. The areas where misfit dislocations locate underneath are stressed, whereas those regions between neighboring misfit dislocations are unstressed or less stressed. With further growth, the adatoms on the film surface will transport from the stressed regions to the unstressed regions through a surface diffusion process. As a result, an island-like surface is formed, as shown in Fig. 5(c) (comparing with Fig. 1). The formation of these islands on the surface will further reduce the strain energy in the film.

Furthermore, our TEM observations also showed that while a $SrRuO_3$ film grown on (001) $SrTiO_3$ consists of only the [110] oriented domains, a film grown on (001) $LaAlO_3$ is composed of all three types of domains. Recent *in situ* TEM studies suggested that $SrRuO_3$ has a cubic structure at deposition temperature and the domain structures observed in TEM result from the phase transformation from the cubic phase to the orthorhombic phase at room temperature.[18] During the phase transition the formation of orientation domains can release elastic strains in the films. The crystallographic configuration of orientation domains formed in the film will also be influenced by the structure and stress of the film/substrate interface. Therefore, different domain structures are expected in the films grown on the substrates with different degrees of lattice mismatch. The exact domain structure will also depend on many other factors including interfacial bonding, interface orientation, step flaws, defects in both films, and substrates.

V. CONCLUSIONS

To conclude, the present experimental studies showed that $SrRuO_3$ thin films deposited on (001) $LaAlO_3$ substrates by 90° off-axis sputtering at 600 °C have a rough surface and consist of orientation domains (twins) of all three (X,Y, and Z) types. The observed domain structure and the surface morphology are different from the $SrRuO_3$ film deposited on the (001) $SrTiO_3$ substrate which has an atomically flat surface and is composed of only the [110] oriented domains. The reasons for these differences was ascribed as an effect of lattice mismatch across the film/substrate interface. A $SrRuO_3$ thin film grows on a (001) $SrTiO_3$ substrate through a two-dimensional nucleation process, while a film on $LaAlO_3$ grows through the two-dimensional nucleation process at the initial stage, followed by an island-like growth process after the formation of misfit dislocations when the film growth reaches a critical thickness.

ACKNOWLEDGMENTS

The authors are grateful to C. B. Eom at Duke University for providing the samples. This work was supported by the College of Engineering at the University of Michigan and through the National Science Foundation through Grant No. DMR 9973801.

[1] C. B. Eom, R. B. Van Dover, J. M. Phillips, D. J. Werder, J. H. Marshall, C. H. Chen, R. J. Cava, R. M. Fleming, and D. K. Fork, Appl. Phys. Lett. **63**, 2570 (1993).
[2] L. Antognazza, K. Char, T. H. Geballe, L. L. H. King, and A. W. Sleight, Appl. Phys. Lett. **63**, 1005 (1993).
[3] K. Char, M. S. Colclough, T. H. Geballe, and K. E. Myers, Appl. Phys. Lett. **62**, 196 (1993).
[4] X. D. Wu, S. R. Foltyn, R. C. Due, and R. E. Muenchausen, Appl. Phys. Lett. **62**, 2434 (1993).
[5] L. Klein, J. S. Dodge, T. H. Geballe, A. Kapitulnik, A. F. Marshall, L. Antognazza, and K. Char, Appl. Phys. Lett. **66**, 2427 (1995).
[6] W. Bensch, H. W. Schmalle, and A. Reller, Solid State Ionics **43**, 171 (1990).
[7] D. B. Kacedon, R. A. Rao, and C. B. Eom, Appl. Phys. Lett. **71**, 1724 (1997).
[8] Q. Gan, R. A. Rao, and C. B. Eom, Appl. Phys. Lett. **70**, 1962 (1997).
[9] J. C. Jiang, X. Pan, and C. L. Chen, Appl. Phys. Lett. **72**, 909 (1998).
[10] J. C. Jiang, X. Pan, W. Tian, Q. Gan, and C. B. Eom, Appl. Phys. Lett. **72**, 2963 (1998).
[11] C. W. Jones, P. D. Battle, P. Lightfoot, and W. T. A. Harrison, Acta Crystallogr., Sect. C: Cryst. Struct. Commun. **C45**, 365 (1989).
[12] S. Geller and V. B. Bala, Acta Crystallogr. **9**, 1019 (1956).
[13] R. A. Rao, Q. Qan, and C. B. Eom, Appl. Phys. Lett. **71**, 1171 (1997).
[14] C. W. Snyder, B. G. Orr, D. Kessler, and L. M. Sander, Phys. Rev. Lett. **66**, 3032 (1991).
[15] G. L. Catchen, T. M. Rearick, and D. G. Schlom, Phys. Rev. B **49**, 318 (1994).
[16] S. C. Gausepohl, M. Lee, R. A. Rao, and C. B. Eom, Phys. Rev. B **54**, 8996 (1996).
[17] D. J. Sroovitz, Acta Metall. **37**, 621 (1989).
[18] J. C. Jiang and X. Q. Pan, Philos. Mag. Lett. **80**, 271 (2000).